Supporting Information

Electrocatalytic Imprinted Polymer of N-doped Hollow Carbon Nanospheres-Palladium Nanocomposite for Ultratrace Detection of Anticancerous 6-Mercaptopurine

Anil Kumar[1], Purnendu Kumar Pathak[1] and Bhim Bali Prasad[*]

Analytical Division, Department of Chemistry, Institute of Science,
Banaras Hindu University, Varanasi-221005, India.

E-mail address: prof.bbpd@yahoo.com (B. B. Prasad)
Fax: +91 542 22368127, Tel: +91 9451954449,

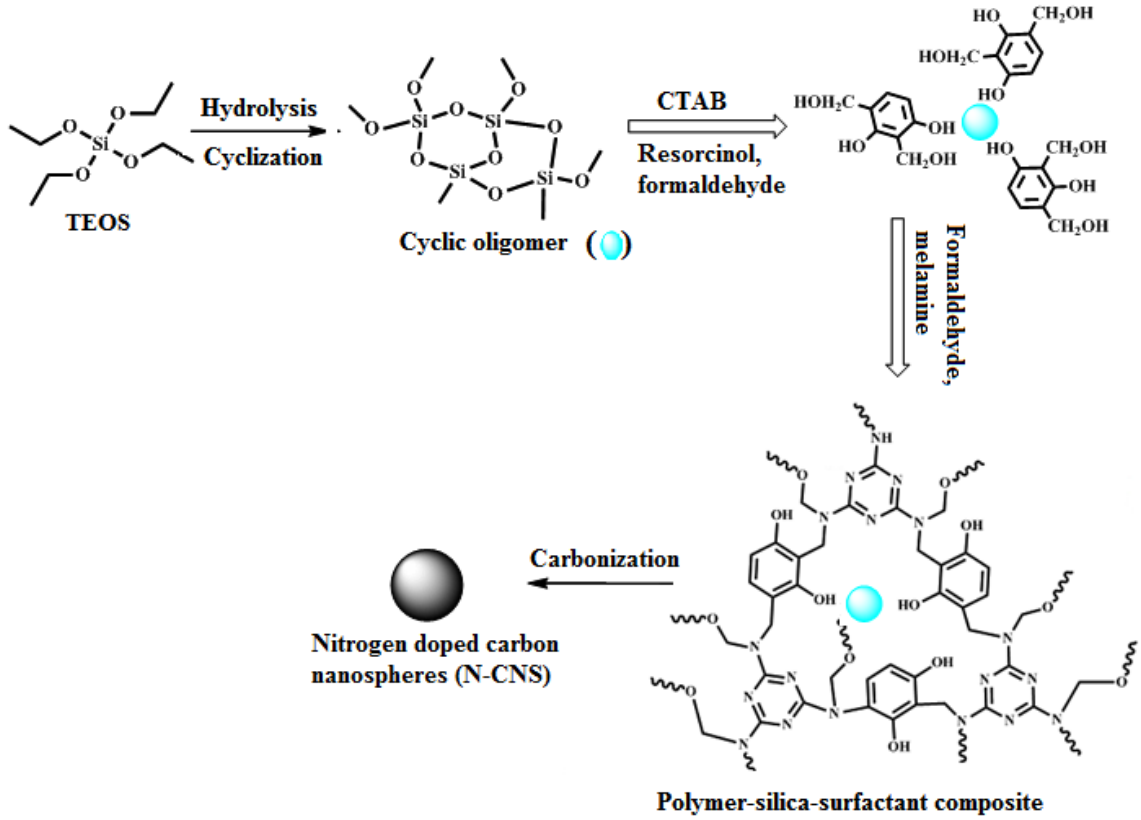

Scheme S1. Schematic representation for the formation of N-CNS.

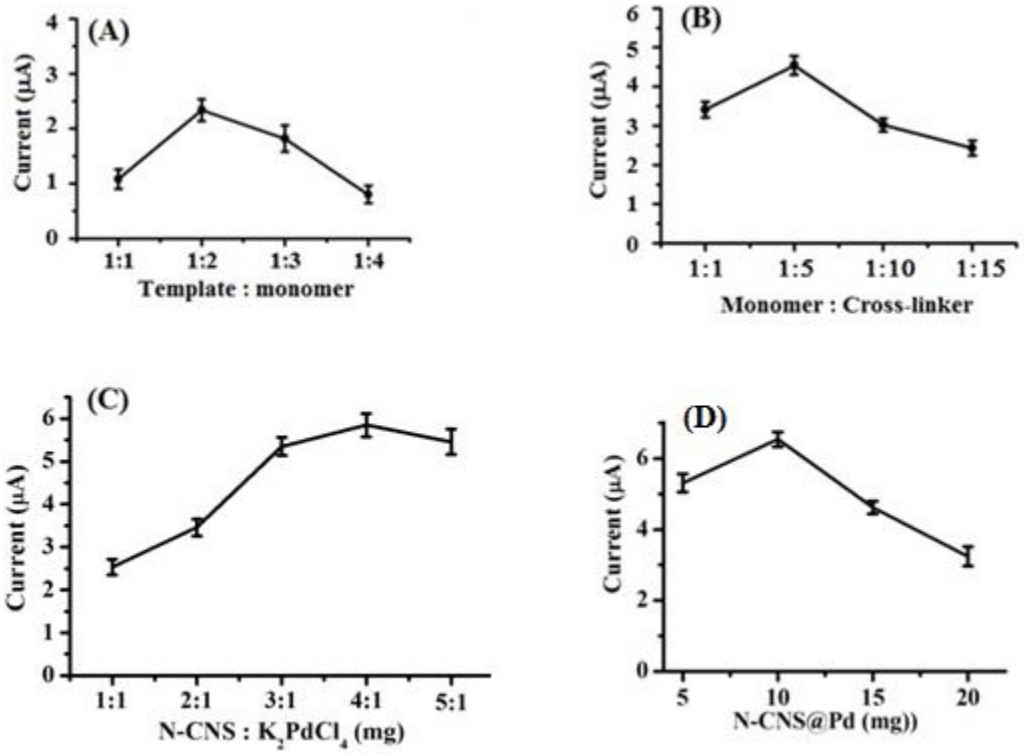

Figure S1. Effect of template: monomer molar ratio (A), monomer cross-linker molar ratio (B), N-CNS: K_2PdCl_4 weight ratio (C), and amount of N-CNS@Pd (D) on DPASV response of 6-MP.

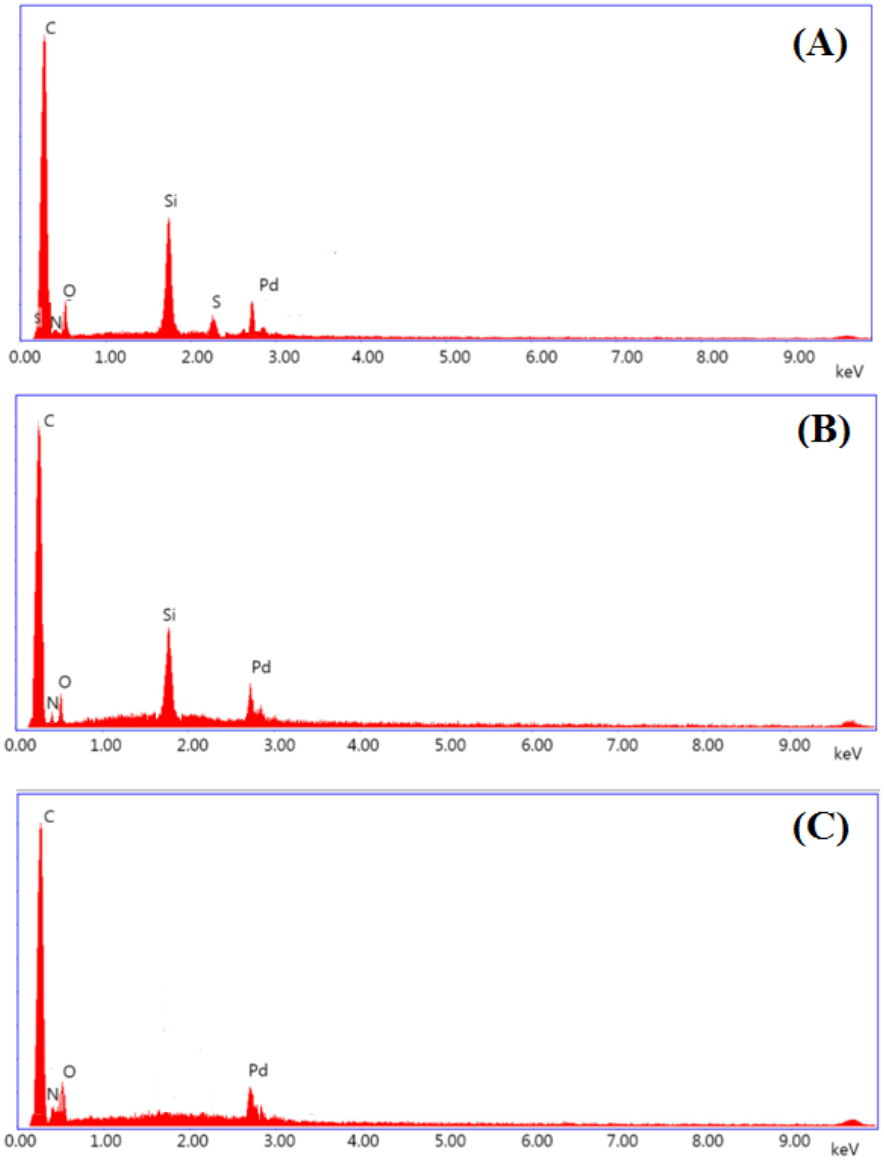

Figure S2. EDS spectra: (A) N-CNS@Pd-MIP-adduct, (B) N-CNS@Pd-MIP, and (C) N-HCNS@Pd-MIP.

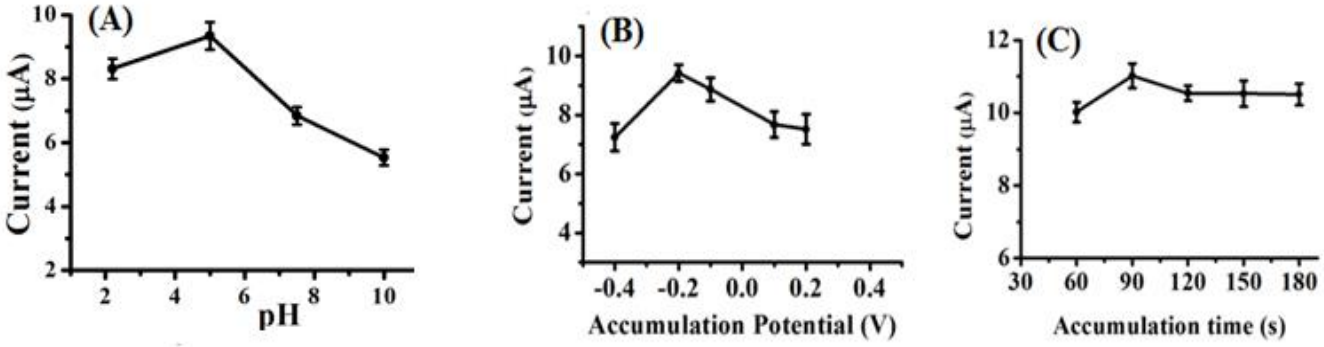

Figure S3. Effect of pH of supporting electrolyte (A), accumulation potential (B), and accumulation time (C) on DPASV response of 6-MP.

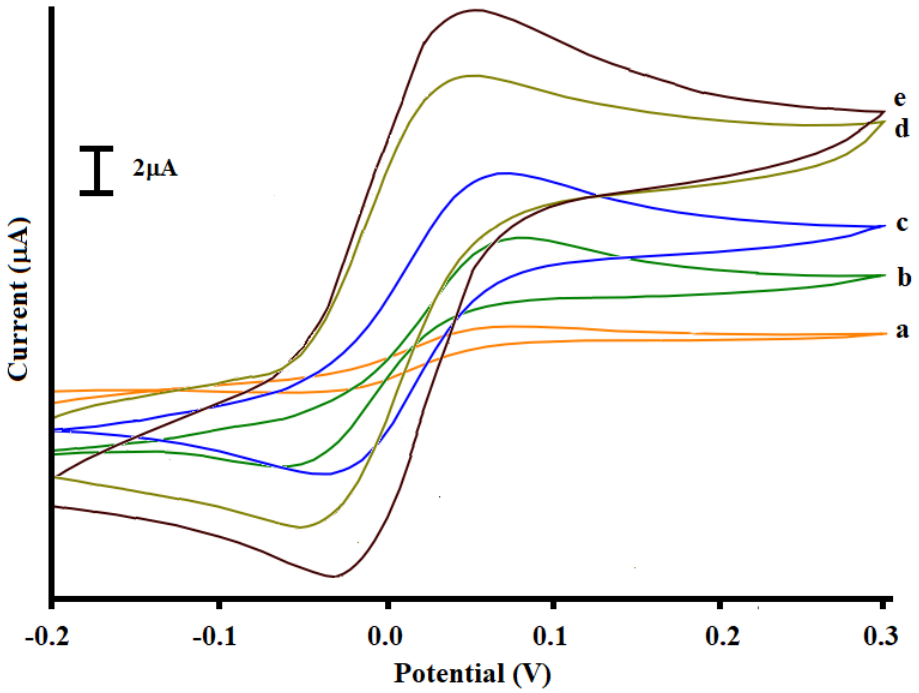

Figure S4. CV runs showing electrochemical behavior of potassium ferricyanide probe (0.1 mM) on (a) IL-PGE (b) N-CNS/IL-PGE, (c) N-CNS@Pd/IL-PGE, (d) N-CNS@Pd-MIP/IL-PGE, and (e) N-HCNS@Pd-MIP/IL-PGE in phosphate buffer solution (pH 5.0, 0.1 M), scan rate = 100 mVs^{-1}.

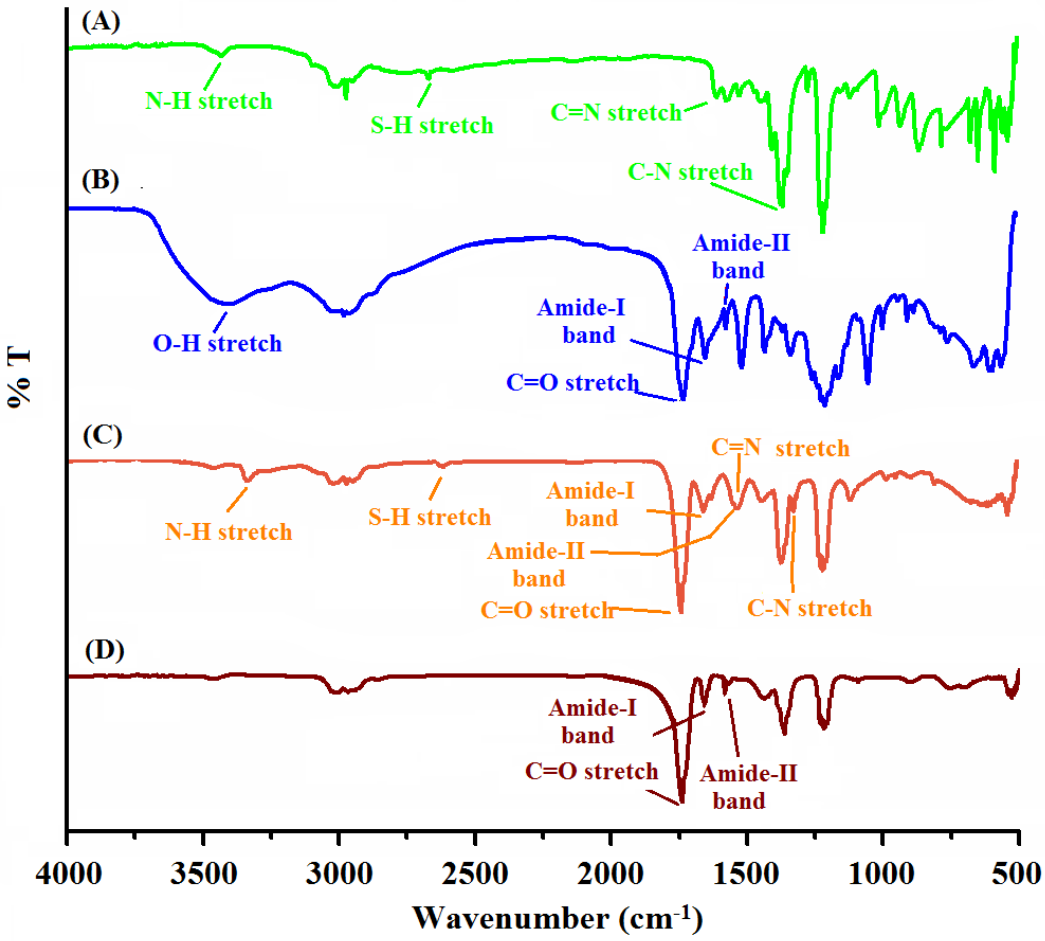

Figure S5. FT-IR (KBr) spectra of template (A), monomer (B), MIP-adduct (C), and MIP (D).

Table S1. The Selectivity Coefficients (*k*), Relative Selectivity Coefficients (*k′*), and Imprinting Factor (*I.F.*) values obtained on N-HCNS@Pd-MIP/IL-PGE and N-HCNS@Pd-NIP/IL-PGE

Compound	I_{MIP} (μA)	I_{NIP} (μA)	k_{MIP}	k_{NIP}	k'	*I.F.*
6-MP	11.04	0.64	-	-	-	17.250
CHB	0.40	0.60	0.036	0.937	0.038	0.660
IFO	0.42	0.68	0.038	1.062	0.023	0.617
TMZ	0.36	0.84	0.032	1.312	0.043	0.428
5-FU	0.42	0.56	0.038	0.875	0.043	0.750
6-TG	0.76	0.86	0.068	1.343	0.050	0.813
AA	0.44	0.52	0.039	0.812	0.048	0.846
DA	0.24	0.50	0.021	0.781	0.026	0.600
Glu	0.28	0.60	0.025	0.937	0.026	0.466
UA	0.36	0.48	0.027	0.45	0.060	0.750

k = selectivity coefficient was calculated as $i_{interferent}/i_{6\text{-}MP}$ (μA).
k' = relative selectivity coefficient was calculated as k_{MIP}/k_{NIP}.
$I.F. = i_{MIP}/i_{NIP}$

Supporting Information Section

S.1

To study the stoichiometric effect on polymerization, different template to monomer molar ratios (1:1, 1:2, 1:3 and 1:4) were investigated (Figure S1A). The 1:2 molar ratios of template and monomer responded the maximum DPASV response of 6-MP. The molar ratios <1:2 revealed lower response owing to decline in the number of binding sites in the absence of an adequate amount of template molecules. On the other hand, molar ratios >1:2 produced low response due to probable heterogeneity of binding sites in the presence of an excess amount of monomer. The stoichiometry of template-monomer complex could further be supported by using the following equation.[1]

$$\frac{1}{i_p} = \frac{1}{i_p max} + \frac{1}{i_p max \ \beta \ C_t^m} \qquad (1)$$

where i_p is the measured peak current, $i_{p.}max$ the peak current when all template molecules formed complex with monomer, C_t the concentration of template, m is the coordination number of the complex formed between template (6-MP) and monomer (N-AAsp), and β is the stability constant. On substituting m = 1, 2, 3 and 4 in the above equation, the respective $1/i_p$ *vs* $1/C_t^m$ plots showed linearity with the coefficient of variation (R^2) 0.94, 0.99, 0.98 and 0.96, respectively. Herein, m = 2 yielded perfect linearity, clamming 1:2 (template: monomer molar ratio) ratio to be an optimized formulation of MIP. The optimum amount of cross-linker (N,N-MBA) for MIP synthesis revealed the specific stabilized binding sites with requisite rigidity and porosity of entire network (Figure S1B) to ensure maximum DPASV current at 1:5 molar ratios of monomer and cross-linker. The gradual decreasing response above this amount of cross-linker (1:10 and 1:15 molar ratios) could apparently be due to the high rigidity of polymer matrix which restricted the accessibility of analyte molecules toward recognition sites. On the other hand, 1:1 molar ratio (monomer: cross-linker) led the formation of un-stabilized and flexible binding sites in polymer matrix, which diminished the current response. For the preparation of N-CNS@Pd, optimized amount of N-CNS and K_2PdCl_4 (4:1, w/w) were utilized which responded maximum DPASV response (Figure S1C). Interestingly, the 10.0 mg of N-CNS@Pd hybrid in prepolymer solution responded highest DPASV current for 6-MP (Figure S1D). Beyond this amount of

hybrid, the heterogeneity in recognition sites might be experienced which declined the current response. At the lower amount of hybrid, the current response was also decreased presumably due to an ineffective electrocatalytic action along with the poor porosity and conductivity.

S.2

For DPASV measurement in this work, various parameters, *viz.*, pH, accumulation potential (E_{acc}), and accumulation time (t_{acc}) were optimized (Figure S3). The DPASV peak current was gradually increased until it reached to a maximum at pH 5.0 and then-after decreased. A plausible explanation to this event may be accorded with pKa value of 6-MP. Accordingly, amine group (pKa 7.72)[2] of 6-MP can be protonated at 5.0 pH. The protonated 6-MP thus produced experiences electrostatic interactions with negatively charged electrode for better rebinding. Such interactions are not feasible at ≥ pH 7.7, since 6-MP is in neutral or anionic form in basic media. The DPASV responses were gradually decreased at pH < 5.0 due to the probable electrode fouling in strong acidic media. Insofar as E_{acc} is concerned, the maximum development of DPASV current for 6-MP (50 ng mL^{-1}) was observed at -0.2 V vs. Ag/AgCl. Any potential higher and lower than -0.2 V, responded diminishing current due to apparent electrode-electrolyte repulsion and steric-crowding amongst 6-MP molecules, respectively. Furthermore, DPASV peak height was progressively increased up to 90 s (t_{acc}) and then slowly decreased presumably due to the destabilization of molecular cavities after binding sites saturation.

S.3

Figure S5, shows a comparative study of 6-MP, N-AAsp, MIP-adduct, and MIP using FT-IR (KBr) to reveal the binding mechanism between MIP (host) and 6-MP (guest) (Scheme 1). Accordingly, typical bands of the 6-MP in curve a [N-H (3421 cm^{-1}), S-H (2671 cm^{-1}), C=N (1612 cm^{-1}) and C-N (1370 cm^{-1})] are shifted downward to 3330, 2615, 1530 and 1320 cm^{-1}, respectively. Notably, the characteristics bands of N-AAsp in curve b [amide-II band (1573 cm^{-1}) are also found to be shifted downward to 1530 cm^{-1} owing to hydrogen bondings between monomer and template to form adduct (curve c). Notably, other two characteristic peaks of N-AAsp [C=O (1732 cm^{-1}) and amide-I (1650 cm^{-1}) remained unaffected upon complexation. The disappearance of OH peak (at 3414 cm^{-1}) of N-AAsp upon MIP-adduct formation revealed the deprotonation of acidic group in aqueous medium. It may be noted that for MIP formation with

retrieval of template molecules the characteristic peak (S-H at 2671 cm^{-1}) of 6-MP are completely disappeared. This also supported the complete template removal.

S.4

For BET analysis of N-CNS@Pd-MIP and N-HCNS@Pd-MIP, 100 mg sample was placed in a sample holder and degassed at 100 ^{o}C for 5 h. Values obtained from the nitrogen desorption step were used to compute the specific surface area. The specific surface areas of N-CNS@Pd-MIP and N-HCNS@Pd-MIP were observed as 113.24 m^2 g-^{1} and 136.17 m^2 g^{-1}, respectively. The higher specific surface area of N-HCNS@Pd-MIP reflects an exclusive role of porous hollow core texture of MIP nanocomposite.

In order to measure the swelling characteristics of N-CNS@Pd-MIP and N-HCNS@Pd-MIP, 50 mg of each MIP nanocomposite were suspended in 1.5 mL of water with vigorous shaking (5 min), followed by an equilibration for 5 h. Afterward, the weight of the wet MIP nanocomposite was measured after filtering the product and removing the excess of solvent. The percent swelling ratio is calculated using the following equation:

$$\%\,Swelling\ ratio = \frac{(M_w - M_d)}{M_w} \times 100 \qquad (\mathbf{2})$$

where M_w is the mass of the wet polymer and M_d is the mass of the dry polymer. The swelling ratios of N-CNS@Pd-MIP and N-HCNS@Pd-MIP in water are found to be 38.6 and 53.4 %, respectively.

S.5

Conductivities of N-CNS@Pd-MIP and N-HCNS@Pd-MIP were measured at a particular voltage range (+10 to -10 V) using the two-point probe method, on the basis of the following equation:

$$\rho = \frac{1}{R} \times \frac{l}{a} \qquad (3)$$

where 'ρ' is conductivity, 'l' is the thickness, 'a' is the area, and 'R' is the mean resistance. Accordingly, N-HCNS@Pd-MIP demonstrated higher conductivity (1.54×10^{-3} S cm^{-1}) than the N-CNS@Pd-MIP (1.34×10^{-4} S cm^{-1}).

S.6

The surface coverage concentration (Γ^0) and diffusion coefficient (D) of the analyte were calculated with the help of chronocoulometry studies. The relationship between Q and $t^{1/2}$ (Anson plots) can be described by integrated Cottrell equation[3] as follows:

$$Q = 2nFAC(Dt)^{1/2}\pi^{-1/2} + Q_{ads} + Q_{dl} \quad (4)$$

$$Q_{ads} = nFA\Gamma^0 \quad (5)$$

where A is the electrochemical surface area of the electrode (1.16 cm^2), C the concentration (1.3×10^{-7} mole L^{-1}) of 6-MP, Q_{dl} the double layer charge, and Q_{ads} is the faradic oxidative charge; other symbols have their usual meanings. For MIP nanocomposite modified IL-PGEs, Q_{dl} and total charge ($Q_{dl} + Q_{ads}$) are obtained from the intercepts of the Anson plots (Q vs. $t^{1/2}$) in the absence and presence of 6-MP, respectively. Surface coverage can be obtained in terms of number of electron 'n' by the equation defining Nerstian adsorbent layer:[4]

$$I = \left[\frac{n^2F^2}{4RT}\right] \Gamma^0 Av \quad (6)$$

Accordingly, n is found to be 1.8. The Γ^0 values were obtained to be 5.38×10^{-12} and 1.99×10^{-11} mol cm^{-2} for N-CNS@Pd-MIP/IL-PGE and N-HCNS@Pd-MIP/IL-PGE, respectively. This suggested the total surface coverage of specifically bound analyte molecules 3.98×10^{-12} mol or 23.97×10^{10} molecules and 2.3×10^{-11} mol or 13.90×10^{12} molecules of 6-MP for N-CNS@Pd-MIP/IL-PGE and N-HCNS@Pd-MIP/IL-PGE, respectively. From the slope of the Anson plots, 'D' values for 6-MP are calculated as 1.04×10^{-4} and 3.76×10^{-4} cm^2 s^{-1} at N-CNS@Pd-MIP/IL-PGE and N-HCNS@Pd-MIP/IL-PGE, respectively.

We have also calculated electron transfer rate constant (k) by using the Velasco equation:[5]

$$k = 1.11D^{1/2}/\left(E_p - E_{p/2}\right)^{-1/2} v^{1/2} \quad (7)$$

The k values for 6-MP at N-CNS@Pd-MIP/IL-PGE and N-HCNS@Pd-MIP/IL-PGE are observed to be 5.06×10^{-3} and 9.62×10^{-3} cm s^{-1}. This indicates a fast electro-oxidation kinetics of 6-MP in the phosphate buffer (pH 5.0).

S.7

Spontaneity of the linear adsorption of analyte in MIP cavities can be investigated on the basis of the Langmuir adsorption isotherm:[6]

$$\theta = \frac{bc}{1 + bc} \tag{8}$$

where θ is the ratio of the surface coverage 'Γ^0' at any concentration 'C' to its maximum surface coverage Γ^{max}. The equation (8) can be rearranged as

$$\frac{C}{\Gamma^0} = \frac{1}{b\,\Gamma^{max}} + \frac{C}{\Gamma^{max}} \tag{9}$$

Thus, a linear equation, $C/\Gamma^0 = (0.865 \pm 0.04) \times 10^{11}\, C + (4.72 \pm 0.75)$ ($R^2 = 0.99$), for the plot of C/Γ^0 vs. C is obtained. The intercept of this equation suggested an estimate of adsorption coefficient (b) to be 1.83×10^{10} L mol^{-1}. The Gibbs free energy change ($\Delta G = -RT\ ln\ b$) due to analyte adsorption could be calculated as – 58.56 kJ mol^{-1}. The negative ΔG value suggested the spontaneous analyte adsorption in the molecular cavities, without any mutual interaction.

References:

(1) Gao, X. Handbook on the Physics and Chemistry of Rare Earth. **1986**, 8, 63–201.

(2) Jayant, I. G.; Mallappa, M.; Sharanappa, T. N. CTAB Functionalized Multiwalled Carbon Nanotube Composite Modified Electrode for the Determination of 6-Mercaptopurine. *Sens. Bio-Sens. Res.* **2017**, 12, 1–7.

(3) Bard, A. J.; Faulker, L. R. Electrochemical Methods 2nd ed. Wiley, New York, 47, **2001**.

(4) Hassen, W.; Martelet, C.; Davis, F.; Higson, S.; Abdelghani, A.; Helali, S. Calix[4]arene based Molecules for Amino-acid Detection. *Sens. Actuators B-Chem.* **2007**, 124, 38–45.

(5) Velasco, J. G. Determination of Standard Rate Constants for Electrochemical Irreversible Processes from Linear Sweep Voltammograms. *Electroanalysis* **1997**, 9, 880–882.

(6) Ju, H.; Leech, D. Electrochemical Study of a Metallothionein Modified Gold Disk Electrode and its Action on Hg^{2+} Cations. *J. Electroanal. Chem.* **2000**, 484, 150–156.